Determination of the absolute sign of nuclear quadrupole interactions by laser radio-frequency double-resonance experiments

Tilo Blasberg and Dieter Suter
Institute of Quantum Electronics, Swiss Federal Institute of Technology (Eidgenössische Technische Hochschule) Zürich, CH-8093 Zürich, Switzerland
(Received 25 June 1993)

The interaction between the quadrupole moment of nuclear spins $I > \frac{1}{2}$ with the electric-field-gradient (EFG) tensor leads to a splitting of the energy of the nuclear spin states. We show how the combination of laser and radio-frequency irradiation allows measurements of nuclear spin transitions in quadrupolar systems that are, in contrast to purely magnetic experiments, sensitive to the *absolute sign* of the quadrupole interaction. This determination of the sign is essential for comparison with calculated EFG tensors.

The coupling between the nuclear quadrupole moment and the electric-field-gradient tensor is, besides the Zeeman effect, the most important interaction of nuclear spins $I > \frac{1}{2}$ with their environment.[1] Since this coupling depends strongly on the electronic environment of the nucleus, it is a sensitive probe for the structure of solids[2] and, through its effect on spin relaxation, also of motional processes. Determination of the nuclear quadrupole coupling tensor has, therefore, often been an important tool in magnetic resonance investigations of crystalline, powdered, or amorphous materials. Comparison of the measured values with theoretically calculated data can serve as a check for electronic-structure calculations or as a tool for measuring atomic polarizabilities.[3] The main experimental tool for the determination of quadrupole coupling constants is nuclear magnetic resonance (NMR) in high magnetic fields[4] and its low-field relative, nuclear quadrupole resonance (NQR). These methods can provide very precise data on the magnitude of the quadrupole coupling constants; however, they are insensitive to its sign; multiplication of the quadrupole coupling Hamiltonian with -1 has no effect on the observed magnetic resonance spectrum obtained by any combination of static and oscillatory magnetic fields, as long as the high-temperature approximation for the nuclear-spin system is valid.[5] It is, therefore, necessary to reduce the spin temperature to $T < 10$ mK to determine the sign by nuclear magnetic resonance.[6]

Experiments of this type have been performed by cooling the nuclear-spin reservoir through dynamic nuclear polarization. The nuclear spins are, therefore, not in thermal equilibrium with the lattice and the sign information must be extracted through an analysis of the observed line shape. The interpretation of the experimentally observed spectra depends on an understanding of the relevant relaxation processes; in the past, this indirect procedure has led to discrepancies between measurements performed in different laboratories.[7,8] In favorable cases, it is possible to measure the sign of the coupling constant relative to other quantities. As an example, it was shown that the two different sites of Li in Li_3N have opposite signs;[9] the absolute sign, however, is still unknown. In the case of Al_2O_3, a partly resolved dipole interaction between two ^{27}Al nuclei allowed the determination of the sign relative to the dipole interaction,[10] which can be calculated from the geometry. Theoretical calculations of the quadrupole coupling constant include the sign information and can be used to check the experimental results. However, the accuracy of the theoretical results is often not sufficient for an unambiguous assignment.[11] Furthermore, since the calculated EFG value results from a difference of various contributions, deviations in the magnitude of the individual terms may result in a wrong sign.

Alternative methods for experimental measurements of the sign must break the symmetry of the magnetic interaction Hamiltonian by coupling the nuclear spin to other systems. In paramagnetic systems, the electron spin, coupled by the hyperfine interaction, can represent such a reference system.[12] Another possibility, which can also be used in diamagnetic systems, consists in coupling the system to an additional state, e.g., by an optical transition to an electronically excited state. Figure 1 shows schematically for the case of a spin $I = \frac{5}{2}$, how such an experiment can determine the quadrupole coupling con-

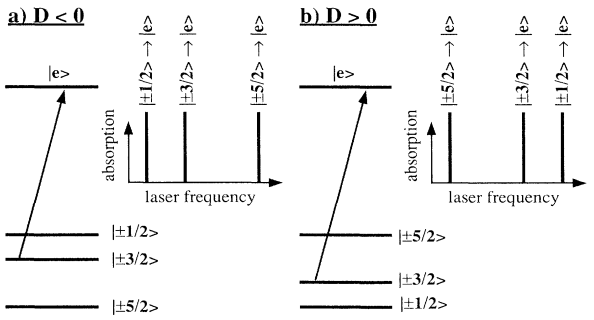

FIG. 1. Principle of measurement of nuclear quadrupole splitting by high-resolution laser spectroscopy. $|e\rangle$ represents an electronically excited state. The left- (right-) hand part of the figure shows, in the form of a stick spectrum, the resulting optical absorption for negative (positive) quadrupole coupling.

stant. Assuming an axially symmetric environment, we write the zero-field nuclear-spin Hamiltonian as $\mathcal{H}_Q = DI_z^2$, where the coupling constant depends on the electric-field-gradient tensor V at the site of the nucleus as $D = 3eQV_{zz}/[4I(2I-1)]$ (Ref. 1). Here, Q represents the nuclear-quadrupole moment, I the nuclear spin, and e the elementary charge unit. This Hamiltonian has two sets of eigenstates corresponding to the I_z eigenstates with magnetic quantum numbers $\pm\frac{5}{2}\pm\frac{3}{2}$, and $\pm\frac{1}{2}$. As shown in Fig. 1, the energies of these states appear directly as frequency shifts in the optical-absorption spectrum.

Obviously, such a direct optical determination of the energy difference between the different spin states is possible only if the frequency resolution is high enough; the width of the optical resonance line must be smaller than the quadrupole interaction. Unfortunately, this is often not the case, since inhomogeneous broadening mechanisms due to crystal strain usually exceed the size of the quadrupole interaction by several orders of magnitude. Several methods exist that can overcome this problem and lead to high-resolution spectra, which are limited, in principle, only by the homogeneous width of the nuclear-spin transition. Examples include spectral hole burning[13] and Raman heterodyne detection of magnetically excited resonances.[14,15] While these methods do provide high resolution, allowing a precise determination of the quadrupole coupling constants, the sign information is lost. In the Raman heterodyne experiment, the same limitations apply as for purely magnetic experiments. For the hole-burning experiments, we demonstrate the problem in Fig. 2; the transmitted intensity does not depend on the sign of the difference between the pump- and test-laser frequencies. It is, therefore, in most cases not feasible to extract the sign information unambiguously.

Optical spectroscopy alone is, therefore, also insufficient for the determination of the quadrupole coupling constant. However, the combination of laser spectroscopy and magnetic resonance permits the determination of all relevant parameters, including the sign information. Figure 3 shows schematically the experimental

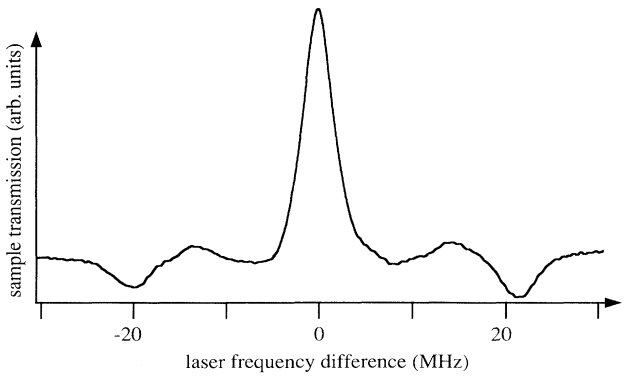

FIG. 2. Example of a hole-burning spectrum of Pr^{3+} in $YAlO_3$: The transmitted intensity is plotted as a function of the difference between the frequencies of the test- and pump-laser beams.

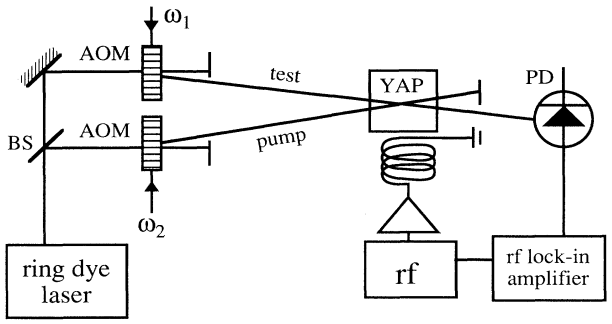

FIG. 3. Schematic representation of the experimental setup. BS=beam splitter, AOM=acousto-optic modulator, rf=radio-frequency synthesizer, PD=photodiodes.

setup that we use for this purpose. It consists of the basic Raman heterodyne scheme,[14] modified by the addition of a pump-laser beam. Two acousto-optic modulators, which are driven by tunable radio-frequency sources with frequencies ω_1 and ω_2, shift the frequencies of the test- and pump-laser beams to $\nu_T = \nu_{\text{Las}} - 2\omega_1/2\pi$ and $\nu_P = \nu_{\text{Las}} - 2\omega_2/2\pi$. A third radio-frequency source drives the $(\pm\frac{1}{2}\leftrightarrow\pm\frac{3}{2})$ nuclear-spin transition through direct rf irradiation at $\omega_{\text{rf}}/2\pi = 7.05$ MHz. The Raman heterodyne signal is observed with a fast photodiode and the amplified signal is measured with a lock-in amplifier driven by ω_{rf}.

Figure 4 uses a simplified level scheme to show schematically the principle of two-beam Raman heterodyne spectroscopy. The levels labeled $|0\rangle, |1\rangle$, and $|2\rangle$ are sublevels of the electronic ground state and $|e\rangle$ represents an electronically excited state (we neglect the

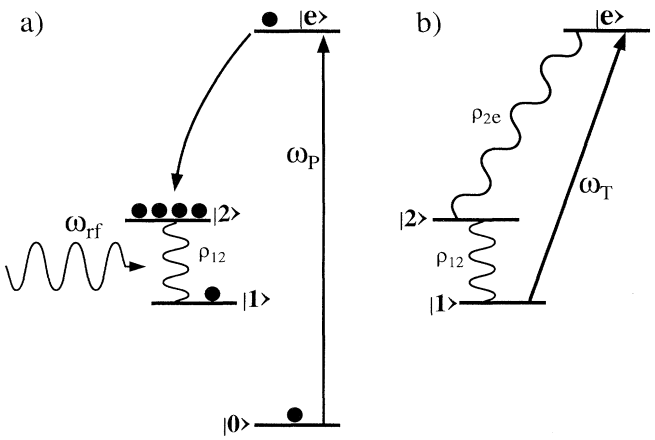

FIG. 4. Principle of two-beam Raman heterodyne spectroscopy. States $|0,\rangle|1\rangle, |2\rangle$ are sublevels of the electronic ground state, $|e\rangle$ represents an electronically excited state. (a) The pump-laser field modifies the ground-state sublevel populations by spectral hole burning. The radio-frequency field excites a coherent superposition of the two unequally populated sublevels $|1\rangle$ and $|2\rangle$. (b) The test-laser field, interacting with the coherent superposition, creates a coherent Raman field in transition $|2\rangle \leftrightarrow |e\rangle$.

quadrupole splitting of the electronically excited state). In the left-hand diagram, Fig. 4(a), the pump laser, which is resonant with the transition between the ground-state sublevel $|0\rangle$ and the electronically excited state $|e\rangle$, redistributes the populations of the ground-state sublevels through spectral hole burning. Depending on the relaxation processes, it excites a population difference between, e.g., states $|1\rangle$ and $|2\rangle$. The radio-frequency (rf) field $\omega_{\rm rf}$, which is resonant with this transition, excites a coherent superposition of these two states. For small rf field-strength and resonant irradiation, the resulting sublevel coherence ρ_{12} is proportional to the population difference $\rho_{22}-\rho_{11}$ as follows:

$$\rho_{12}=iB_{\rm rf}\mu_{12}(\rho_{22}-\rho_{11})/2\hbar\gamma_{12}\ , \tag{1}$$

where $B_{\rm rf}$ represents the rf amplitude, μ_{12} the (magnetic) dipole matrix element for the transition $|1\rangle\leftrightarrow|2\rangle$, and γ_{12} the dephasing rate of the sublevel coherence. The resulting coherent superposition of the two ground-state sublevels can cause a coherent Raman process,[16] if the test-laser field is resonant with the transition between one of the two levels and the excited state; in the figure, we have assumed resonance with the transition $|1\rangle\leftrightarrow|e\rangle$. For a small intensity of the test-laser field, the Raman process creates an optical coherence,

$$\rho_{2e}=-i\rho_{21}\mu_{1e}E_T/(2\hbar\gamma_{2e})\ , \tag{2}$$

where E_T is the amplitude of the test-laser beam and μ_{1e} the (electric) dipole moment of transition $|1\rangle\leftrightarrow|e\rangle$. The corresponding Raman field propagates together with the test-laser beam. On the detector, the two fields interfere to produce a signal beating at the rf frequency. The amplitude of the component at $\omega_{\rm rf}$ is then

$$S_{\rm rf}\propto\mu_{12}\mu_{1e}\mu_{2e}(\rho_{22}-\rho_{11})|E_T|^2B_{\rm rf}/(\gamma_{12}\gamma_{2e})\ . \tag{3}$$

As in the usual Raman heterodyne experiment,[14] the signal is proportional to the product of the matrix elements of the three transitions involved, to the intensity of the test-laser beam, and to the rf amplitude. In contrast to the conventional case, however, only those atoms contribute to the signal that are simultaneously excited by the pump-laser beam. This difference is best appreciated by taking the inhomogeneous broadening of the optical transition into account. In the conventional case, the Stokes and anti-Stokes processes contribute equally to the Raman signal. The resulting spectrum is, therefore, independent of the sign of the quadrupole interaction. In the two-beam Raman experiment, however, only those atoms contribute to the signal that interact simultaneously with both laser fields, and with the rf field. For a given laser-frequency difference, we observe only one of the two contributions and the signal becomes asymmetric.

In Fig. 5, we summarize this situation for the two possible signs of the quadrupole coupling. The stick spectra at the top indicate qualitatively the expected Raman heterodyne signal amplitude as a function of the *difference* $\nu_T-\nu_P$ between the frequency ν_T of the test-laser beam and the frequency ν_P of the pump-laser beam. With the rf field, we excite a transition between two

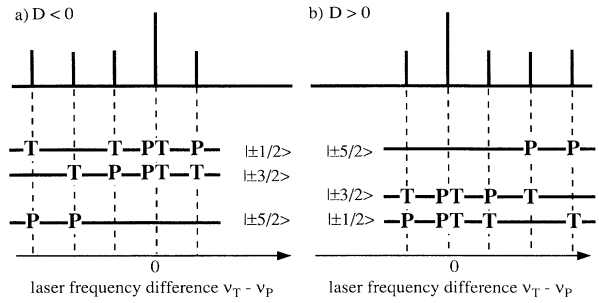

FIG. 5. Theoretical spectra for negative (left) and positive (right) quadrupole coupling. For each resonance line, the letters indicate the spin substates that are in resonance with the pump (P) and test (T) laser frequency.

ground-state sublevels (in our experiment the $m_I=\frac{1}{2}$ and $m_I=\frac{3}{2}$ states); only those atoms for which the test-laser beam is resonant with a transition from one of these states to an excited state, contribute to the observed signal. With two electronic transitions to which the test-laser beam can couple, and three transitions that can be excited by the pump-laser beam, we expect a total of six signal components. In the lower part of Fig. 5, the letters P and T indicate the ground-state sublevels that are simultaneously in resonance with the two laser beams for the given frequency difference. In two cases, pump and test frequencies coincide, while the four other cases occur at clearly distinct frequency differences. The comparison between the two cases of opposite sign shows that the reversal of the sign of the quadrupole coupling leads directly to an inversion of the spectrum.

For the experimental implementation of this scheme, we used the $^3H_4$ electronic ground state of Pr^{3+}, which was present in a $YAlO_3$ (YAP) matrix at a concentration of 0.1%. A crystal of size $5\times5\times1$ mm was cooled to 4.4

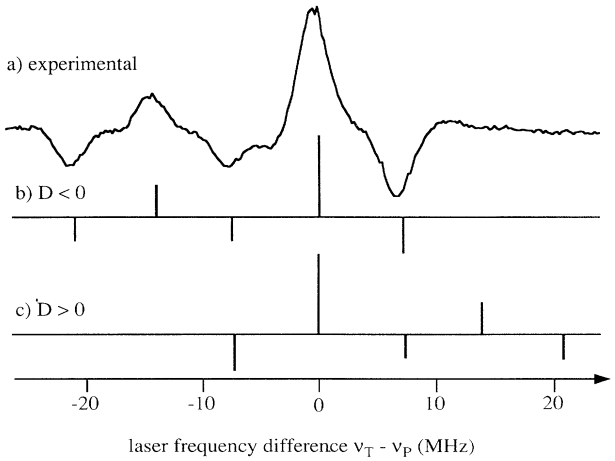

FIG. 6. Experimental spectrum (top) compared to the calculated stick spectra for positive and negative quadrupole coupling. The rf frequency was 7.05 MHz, in resonance with the $\pm\frac{1}{2}\leftrightarrow\pm\frac{3}{2}$ transition.

K in a flow cryostat and the two laser beams propagated along the crystal c axis. The laser frequency was close to the transition between the ground state and the $^1D_2$ excited state ($\lambda = 610.698$ nm). The 7.05 MHz rf field was applied to the crystal through a coil that was part of a tuned circuit; the resulting radio-frequency field strength at the crystal was of the order of 10 μT. The rf frequency was kept on resonance with the nuclear-spin transition for this experiment. Figure 6 shows the resulting heterodyne signal, after demodulation, as a function of the difference of the two laser frequencies, together with the two theoretical stick spectra. The width of the optical resonance lines is dominated by the (unresolved) nuclear quadrupole splitting of the electronically excited state and the laser frequency jitter. The comparison of the experimental spectrum with the two theoretical spectra shows clearly, that the sign of the ground-state quadrupole coupling must be negative.

We have measured the value of the coupling constant independently, by keeping the laser frequencies constant and scanning the radio frequency. At 4.4 K, the center of the resonance line is at 7.049 ± 0.001 MHz, in good agreement with the value 7.062 MHz calculated from the published data[15] which had been obtained at 1.7 K. Therefore, we conclude that the actual coupling is $D/h = -3.510$ MHz.

In conclusion, we have determined the sign of the quadrupole coupling in the $^3H_4$ electronic ground state of the impurity ion Pr^{3+} in $YAlO_3$, using a laser radio-frequency double-resonance method that combines spectral hole burning with a radio-frequency driven Raman heterodyne experiment. This method should be applicable to other spin systems that have an optically accessible transition to an electronically excited state. Since it relies on the asymmetry of the ground-state level system it can be used only for spins $I > \frac{3}{2}$, unless a significant asymmetry of the quadrupole tensor or an external magnetic field lowers the symmetry of the Hamiltonian.

We would like to thank R. Kind for helpful discussions. This work was supported by the Schweizerischer Nationalfonds.

[1]M. H. Cohen and F. Reif, Solid State Phys. **5**, 321 (1957).
[2]E. N. Kaufman and R. J. Vianden, Rev. Mod. Phys. **51**, 161 (1979).
[3]S. Hafner and M. Raymond, J. Chem. Phys. **49**, 3570 (1968).
[4]M. Mehring, *Principles of High Resolution NMR in Solids* (Springer-Verlag, Berlin, 1983).
[5]A. Abragam, *The Principles of Nuclear Magnetism* (Oxford University Press, Oxford, 1961).
[6]P. Boesiger, C. Gabathuler, and E. Brun, Helv. Phys. Acta. **46**, 415 (1973).
[7]R. K. J. S. Lee and V. P. Jacobsmeyer, Phys. Rev. Lett. **21**, 515 (1968).
[8]H. H. Niebuhr, E. E. Hundt, and E. Brun, Phys. Rev. Lett. **21**, 1735 (1968).
[9]D. Brinkman, M. Mali, J. Roos, R. Messer, and H. Birli, Phys. Rev. B **26**, 4810 (1982).
[10]A. H. Silver, T. Kushida, and J. Lambe, Phys. Rev. **125**, 1147 (1962).
[11]L. E. Erickson, Phys. Rev. B **16**, 4731 (1977).
[12]N. T. Son, T. Gregorkiewicz, and C. A. J. Ammerlaan, Phys. Rev. Lett. **69**, 3185 (1992).
[13]S. Voelker, Annu. Rev. Phys. Chem. **40**, 499 (1989).
[14]N. C. Wong, E. S. Kintzer, J. Mlynek, R. G. Devoe, and R. G. Brewer, Phys. Rev. B **28**, 4993 (1983).
[15]M. Mitsunaga, E. S. Kintzer, and R. G. Brewer, Phys. Rev. B **31**, 6947 (1984).
[16]J. A. Giordmaine and W. Kaiser, Phys. Rev. **144**, 676 (1966).